



Jensen, T. T., Potticary, J., Terry, L. R., Bruce Macdonald, H. E., Brandenburg, J. G., & Hall, S. R. (2017). Polymorphism in crystals of bis(4-bromophenyl)fumaronitrile through vapour phase growth. *CrystEngComm*, 19(48), 7223-7228.  
<https://doi.org/10.1039/c7ce01543g>

Peer reviewed version

Link to published version (if available):  
[10.1039/c7ce01543g](https://doi.org/10.1039/c7ce01543g)

[Link to publication record in Explore Bristol Research](#)  
PDF-document

This is the author accepted manuscript (AAM). The final published version (version of record) is available online via RSC at <http://pubs.rsc.org/en/Content/ArticleLanding/2017/CE/C7CE01543G#!divAbstract> . Please refer to any applicable terms of use of the publisher.

## University of Bristol - Explore Bristol Research

### General rights

This document is made available in accordance with publisher policies. Please cite only the published version using the reference above. Full terms of use are available:  
<http://www.bristol.ac.uk/red/research-policy/pure/user-guides/ebr-terms/>

## Polymorphism in crystals of bis(4-bromophenyl)fumaronitrile through vapour phase growth

Received 00th January 20xx,  
Accepted 00th January 20xx

Torsten T. Jensen<sup>a, b</sup>, Jason Potticary<sup>a, c</sup>, Lui R. Terry<sup>a</sup>, Hannah E. Bruce Macdonald<sup>a</sup>, Jan Gerit Brandenburg<sup>d, e</sup> and Simon R. Hall<sup>a, c</sup>

DOI: 10.1039/x0xx00000x  
[www.rsc.org/](http://www.rsc.org/)

### Abstract

Polymorphic selectivity within crystals grown via physical vapour transport (PVT) is dependent on the thermodynamic stabilities of differing molecular conformations and the kinetic regime within the growth apparatus. Crystals of bis(4-bromophenyl)fumaronitrile have been grown for the first time via this method, with the formation of both the conventional polymorph and a new, unforeseen polymorph. Analysis suggests that the conventional form is less thermodynamically stable, with this form crystallising at higher temperature than the newly discovered form due to the release of binding energy of intermolecular interactions during the growth process. Fluorometry reveals the new form to exhibit weaker, red-shifted fluorescence emission owing to greater intermolecular  $\pi$ - $\pi$  overlap.

### Introduction

Physical vapour transport (PVT), in which a powdered sample is sublimed and recrystallised from the vapour phase, is a commonly used method of growing single crystals of organic semiconducting molecules, due to the size and purity of crystals produced when compared with other methods of crystal growth<sup>1</sup>. Multiple polymorphs of the same material can be produced, dependent on the growth conditions, resulting in crystals with starkly different physical properties including electronic transport and optical emission<sup>2</sup>. Thus, an understanding of polymorphism in PVT growth is critical to produce crystals with optimal properties for optoelectronic applications such as transistors, LED's and lasing.

Bis(4-bromophenyl)fumaronitrile (subsequently Br-FN) is a convenient precursor for bis(4-(N-(1-naphthyl)phenylamino)phenyl)-fumaronitrile (NPAFN) and N-methyl-3,4-bis(4-(N-(1-naphthyl)phenylamino)phenyl)maleimide (NPAMLMe), efficient

emitters for non-doped red organic light-emitting diodes<sup>3</sup>. It has also garnered attention for forming single crystals which fluoresce intensely under exposure to ultra-violet light, with comparatively weak emission in solution. This is due to aggregation induced emission (AIE), in which the intramolecular rotations that quench excited states in solution are effectively prevented in the solid state. In Br-FN, the cyano groups force the aromatic rings out of plane in the crystalline state, preventing intermolecular  $\pi$ - $\pi$  stacking and further reducing quenching and increasing luminescence efficiency<sup>4</sup>. Only one polymorph of Br-FN has been documented on the Cambridge Crystallographic Data Centre (CCDC). The previous report on the synthesis and characterisation of Br-FN in the solid state was obtained by crystallisation from solution and reports only a single polymorph being crystallised<sup>3</sup>.

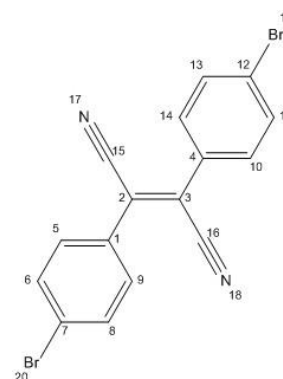


Fig. 1 Chemical structure of bis(4-bromophenyl)fumaronitrile, including atom numbers.

In this work, we synthesise Br-FN via solution and recrystallise from both solution and physical vapour transport (PVT). When

<sup>a</sup> Complex Functional Materials Group, School of Chemistry, University of Bristol, Bristol, BS8 1TS, United Kingdom

<sup>b</sup> Centre for Doctoral Training in Condensed Matter Physics, HH Wills Physics Laboratory, Tyndall Avenue, Bristol, BS8 1TL, United Kingdom

<sup>c</sup> Bristol Centre for Functional Nanomaterials, HH Wills Physics Laboratory, Tyndall Avenue, Bristol, BS8 1TL, United Kingdom

<sup>d</sup> Department of Chemistry, University College London, 20 Gordon Street, London WC1H 0AH, United Kingdom

<sup>e</sup> Thomas Young Centre, University College London, Gower Street, London WC1E 6BT, United Kingdom

† Electronic Supplementary Information (ESI) available: Crystal structure (cif) data for form 1 and form 2 at 100 K, SEM images of grown crystals, pXRD patterns of form 1 crystals extracted from the PVT growth tube, DSC data for form 1 and form 2, Low temperature pXRD data for form 1 and form 2, Crystal data and structure refinement for form 1 and 2, and additional details on DFT calculations. See DOI: 10.1039/x0xx00000x

recrystallising from solution only the previously known polymorph could be obtained, however both the conventional and a new, undocumented polymorph could be grown via PVT at different regions over a temperature gradient within the growth apparatus. Density functional theory (DFT) lattice calculations performed on both polymorphs reveal the two forms to be close in lattice energy, with a slight tendency of the newly discovered form to be more stable, leading us to denote this polymorph as form 2 and the previously documented polymorph as form 1. Form 1 forms at higher temperature to form 2, which is attributed to kinetic factors during growth. Differential scanning calorimetry (DSC) measurements and low temperature powder X-ray diffraction (pXRD) reveal the two forms to be stable within the temperature range 12 to 493 K. Fluorometry shows form 2 to exhibit red-shifted fluorescence when compared to form 1 due to increased intermolecular  $\pi$ - $\pi$  stacking.

## Experimental

### Synthesis

Synthesised as previously reported<sup>3</sup>. 2-(4-Bromophenyl)acetonitrile (0.1 mol) and iodide (0.1 mol) were dissolved in diethyl ether (400 mL) under an inert nitrogen atmosphere. The reaction was cooled to -78 °C and sodium methoxide (0.2 mol) was dissolved in dry and cold methanol, before being added drop-wise to the solution over 30 minutes. The solution was left in a dry ice bath for 2 hours and then an ice bath for the following 3 hours. After this, the solution was stirred for 3 hours at 10 °C before quenching with 3-6% hydrochloric acid. The solution was filtered and the filtrate washed with a cold methanol-water solution. The product was purified using silica gel column chromatography and were separated using methanol, and recrystallized.

### Crystal Growth

**From solution:** A saturated solution of Br-FN in dichloromethane (3 ml) was left to evaporate in an atmosphere of methanol. Crystals spontaneously nucleated from the solution and were collected after eight days when the solvent had completely evaporated.

**Via PVT:** A glass tube (inner diameter 39.5 mm) containing an inner growth tube (inner diameter 17 mm) with bis(4-bromophenyl)fumaronitrile powder placed at one end was inserted into a quartz tube. This was then inserted into a Carbolite CTF horizontal tube furnace such that the powder was positioned at the centre of the furnace. Nitrogen gas was passed through the glass tube at a flow rate of 0.1 L/min. The temperature of the central point of the furnace was set to 240 °C. Crystals formed on the inner walls of the growth tube after 5 hours at distances between 120 and 300 mm from the powder.

**Via vacuum sublimation:** A round bottomed flask with Br-FN powder resting at the bottom was immersed in a sand bath heated to 200 °C with a water-cooled cold finger at 4 °C positioned at the centre of the flask, and the air in the flask was evacuated with a vacuum pump. All

powder had sublimed and recrystallised on the cold finger after 24 hours.

### Fluorometry

Measurements were obtained from an Agilent Cary Eclipse Fluorescence Spectrometer after mounting crystalline samples on the end of a quartz plate using paraffin oil. The quartz plate, cut at an 8° angle, allowed for emitted light to be detected but not directly reflect the incident beam.

### Crystallography

**Powder X-ray diffraction:** pXRD data were gathered using a Bruker D8 Advance diffractometer (Cu-K $\alpha$  radiation - wavelength of 1.5418 Å) with a PSD LynxEye Detector. Step size was 0.0114 2 $\theta$  and hold time was 1 s. Samples were mounted on a low-background sample holder with silicon wafer. Low temperature pXRD: A scan from 7 to 40 2 $\theta$  with a step size of 0.01968 over 41.25 minutes was taken at 300 K. The sample was cooled to 12 K with an Oxford Cryosystems PheniX cryostat as rapidly as possible and was held at 12 K for 15 minutes, after which a scan with the same parameters was taken. The sample was then heated back to 300 K and another scan was taken.

**Single Crystal X-ray diffraction:** Single crystal X-ray diffraction data (SC-XRD) for form 1 and 2 were collected on a Bruker Apex II CCD diffractometer using Mo K $\alpha$  radiation ( $\lambda$  = 0.71073 Å) at a temperature of 100(2) K. Intensities were integrated in SAINT<sup>5</sup> and absorption corrections based on equivalent reflections were carried out using SADABS<sup>6</sup>. The structure was solved using Superflip<sup>7,8</sup> and refined against F2 in ShelXL<sup>9</sup> using Olex2<sup>10</sup>. All of the non-hydrogen atoms were refined anisotropically, while all of the hydrogen atoms were located geometrically and refined using a riding model. Crystallographic and refinement details are available in the supplementary information in Table S1. Crystallographic data for form 1 and 2 have been deposited with the Cambridge Crystallographic Data Centre as supplementary publication CCDC 1568482 and 1563251 respectively. Copies of the data can be obtained free of charge on application to CCDC, 12 Union Road, Cambridge CB2 1EZ, UK [fax(+44) 1223 336033, e-mail: deposit@ccdc.cam.ac.uk].

### Differential scanning calorimetry

DSC data were collected with a TA-Instruments Q100 DSC. 5.3 mg of each sample was hermetically sealed in an aluminium pan and subject to a temperature ramp from 190 °C to 240 °C at a rate of 10.00 °C min<sup>-1</sup>, then ramped back down to 190 °C at the same rate.

### Density Functional Theory

Lattice energy calculations were performed in a developer version of the CRYSTAL14 program package<sup>11</sup>, with a screened exchange hybrid functional (HSE-3c)<sup>12</sup>. The Brillouin zone was sampled with  $\gamma$ -centred grid with 3x3x3 and 6x3x2  $k$ -points for form 1 and form 2, respectively. Standard thresholds were applied for self-consistent

field convergence, geometry optimization and integral screening. The experimental unit cell was used and atomic positions were relaxed within space group constraints. Additional information on DFT calculations available in the supplementary information.

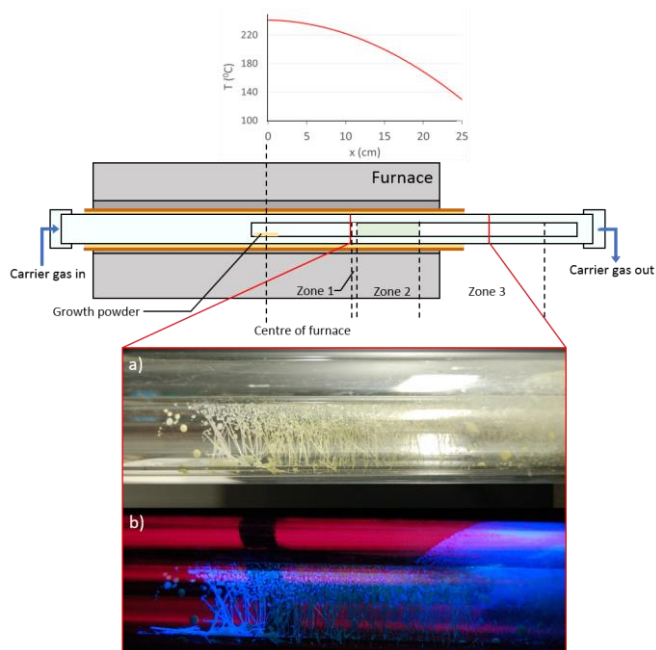


**Fig. 2** Schematic of PVT growth apparatus, including the temperature profile of the furnace. a) crystals grown in the growth tube under lab light, and b) under 365 nm UV light.

## Results and Discussion

Crystals of Br-FN grown via physical vapour transport have needle-like morphology, with sizes ranging from approximately 1 mm to 2 cm in length (Fig. 2). Three distinct “growth zones” appear in the growth tube: a 5 mm zone with a temperature of approximately 210 °C (zone 1), with white needles closest to the Br-FN growth powder which itself was placed at the hottest area of the growth tube; green needles with smaller white crystals over a range of 50 mm with temperatures between 200 °C and 180 °C (zone 2); and a white powder covering the outside of the inner and inside of the outer tube over a 100-mm range (zone 3). Under exposure to 365-nm UV light, the distinction between zones becomes more apparent: intense blue fluorescence is observed from the white crystals and powder, and weaker green emission from the green needles. This is in contrast to solution-grown crystals of Br-FN (Fig. 3), which have a three-dimensional block-like morphology and only fluoresce blue under excitation. SEM images (Fig. S1, ESI<sup>†</sup>) of green PVT-grown needles display smooth, parallel faces, in contrast to the solution-grown crystals which have rough, uneven faces. Vacuum sublimation growth resulted in the formation of a white powder, which fluoresces pale green under UV light (Fig. S2, ESI<sup>†</sup>).

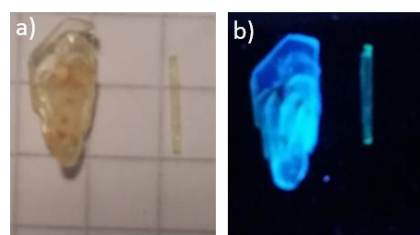


**Fig. 3** Comparison between a solution-grown crystal of form 1 (left) and a PVT-grown crystal of form 2 (right) under a) lab light, and b) 365 nm UV light. Squares are 0.5 cm<sup>2</sup>.

SC-XRD on solvent-grown crystals and pXRD performed on the white crystals and powder from the PVT growth tube matched the pattern of the conventional polymorph (Fig. S3, ESI<sup>†</sup>), subsequently denoted as form 1. This polymorph has a triclinic system with space group *P*-1, and contains two molecules in the unit cell ( $Z' = 1$ ,  $Z = 2$ ). SC-XRD on the green needle-like crystals revealed a novel polymorph which also adopted a triclinic unit cell with space group *P*-1, but had contrasting lattice parameters (Table 1), subsequently denoted as form 2. This polymorph also contains two molecules in the unit cell ( $Z = 2$ ) but this time the asymmetric unit consists of two half molecules ( $Z' = 2 \times 0.5$ ). pXRD of the powder from vacuum sublimation growth matched the calculated pattern from the SC-XRD data of this polymorph (Fig. S4, ESI<sup>†</sup>).

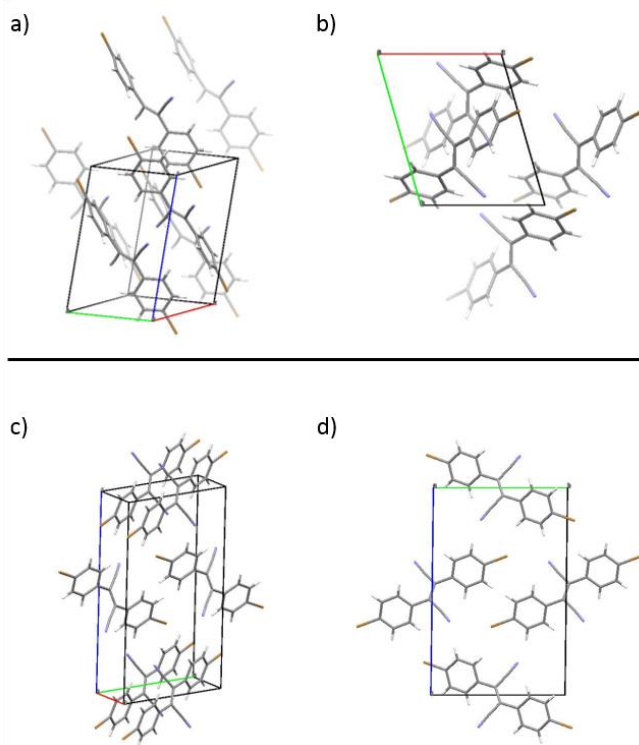


**Fig. 4** a) and b) Crystal structure of the previously known polymorph (form 1) of Br-FN viewed slightly offset from the *a* and *b* axes, and along the *c* axis respectively, with lines representing unit cell boundaries. Depth cueing used to show relative positions of molecules. c) and d) Unit cell of the new polymorph (form 2) viewed slightly offset from the *a* and *b* axes, and along the *a*-axis respectively.

Comparisons between the two forms reveal a starkly different molecular arrangement of Br-FN (Fig. 4). In form 1, the phenyl rings of each molecule are twisted with respect to each other and near-perpendicular with an angle of  $97.83^\circ$  between the mean planes calculated through the carbon atoms of the phenyl rings and a (phenyl)C=C-C(N) torsion angle of  $\sim 8^\circ$ , whereas in the new polymorph (form 2) the rings are parallel with (phenyl)C=C-C(N) torsion angles of  $\sim 2 / -2^\circ$ . Both structures display intermolecular  $\pi$ - $\pi$  stacking interactions which are more extensive in form 2, see Table 1. In form 1 each of the two phenyl rings form one  $\pi$ - $\pi$  interaction to symmetry related phenyl rings on different molecules, creating chains through the structure in approximately the [101] direction. However, in form 2 the parallel orientation of the phenyl rings with respect to each other enables both phenyl rings on each unique molecule to interact with pairs of phenyl rings on parallel molecules above and below with a separation of  $3.87 \text{ \AA}$ , creating  $\pi$ - $\pi$  stacks in approximately the [100] direction, which is aligned with the long axis of the needles. The layered structure is similar to those seen in other derivatives of diphenyl fumaronitriles, such as bis(4-methoxyphenyl)fumaronitrile<sup>3</sup>, whereas the conventionally obtained structure, form 1, is distinctly nonplanar. DSC (Fig. S5 and S6, ESI<sup>†</sup>) reveal that no phase change occurs between the two polymorphs over the temperature range of 300 K to their measured melting points of 493 K. The melting points of the two polymorphs were measured to be equal within error margins, therefore any difference in lattice energy is beyond the detection limits of the DSC apparatus. Low temperature pXRD (Fig. S7 and S8, ESI<sup>†</sup>) performed on powder of form 1 and form 2 also indicate that there is no phase change between 300 K and 12 K. Thus, the polymorphs are monotropic in the temperature range 12 – 493 K. This would therefore suggest the presence of a large potential barrier separating the energy minima of each polymorph. Static (0 K) lattice energy values for the previously known and new forms calculated via DFT (HSE-3c) were  $-148.3 \text{ kJ/mol}$  and  $-151.3 \text{ kJ/mol}$ , respectively. This was confirmed by PBE-D3<sup>13,14</sup> single-point energies on the HSE-3c structures, evaluated in a projector augmented plane wave basis set with energy cut-off of 800eV with the VASP 5.4 code<sup>15</sup> yielding  $-150.2 \text{ kJ/mol}$  and  $-153.8 \text{ kJ/mol}$ . The accuracy of the HSE-3c functional is to within approximately 5 kJ/mol for absolute lattice energies of organic compounds, so both polymorphic forms are equally stable within error values, with a slight tendency of form 2 to be more stable. Form 2 has a 20 kJ/mol higher stabilization from London dispersion forces making it competitive to form 1 and resulting in closer packing, evident in the smaller unit cell volume (Table 2). The similarity in lattice energies would explain how the two polymorphs grow concomitantly in the growth tube.

Form	Ring 1	Ring 2	Centroid-centroid distance (Å)	Offset distance (Å)
1	C1-C6	C1 <sup>1</sup> -C6 <sup>1</sup>	3.70	1.50
	C9-C14	C9 <sup>2</sup> -C14 <sup>2</sup>	4.07	1.25
2	C1-C6	C1 <sup>3</sup> -C6 <sup>3</sup>	3.87	1.39

	C1-C6	C1 <sup>4</sup> -C6 <sup>4</sup>	3.87	1.39
	C9-C14	C9 <sup>3</sup> -C14 <sup>3</sup>	3.87	1.64
	C9-C14	C9 <sup>4</sup> -C14 <sup>4</sup>	3.87	1.64

<sup>1</sup> = -x, 1-y, -z, <sup>2</sup> = 1-x, -y, 1-z, <sup>3</sup> = -1+x, +y, +z, <sup>4</sup> = 1+x, +y, +z

**Table 1**  $\pi$ - $\pi$  stacking interaction distances

The growth of multiple polymorphs of organic crystals in physical vapour transport (PVT) has been reported previously for crystals of 7,14-bis((trimethylsilyl)ethynyl)dibenzo[b,def]-chrysene<sup>16</sup> and  $\alpha$ -quaterthiophene<sup>17</sup>. In these cases, the polymorph that grew at the higher temperature was designated as the “high temperature polymorph” and the polymorph that grew at lower temperature as the “low temperature polymorph”. The temperature of the substrate on which a crystal grows will influence the disturbance of the crystal lattice. A higher temperature substrate will cause the release of binding energy of intermolecular interactions during the growth process<sup>18</sup>. This can therefore lead to the formation of multiple polymorphs dependent on the temperature of the point on the growth tube on which the crystal grows, with less thermodynamically stable polymorphs forming at higher temperature. This matches with our observations that form 1, likely being the less stable of the two polymorphs, forms at higher temperature to form 2. Further evidence arises from the vacuum sublimation growth, with form 2 crystallising on the cold finger at much lower temperatures to the PVT tube.

	Form 1	Form 2
<b>Crystal system</b>	Triclinic	Triclinic
<b>Space group</b>	P -1	P -1
<b>a/Å</b>	7.9926(9)	3.87260(10)
<b>b/Å</b>	9.4626(12)	10.7671(4)
<b>c/Å</b>	10.6914(15)	16.5188(6)
<b><math>\alpha</math>/°</b>	92.131(11)	90.217(3)
<b><math>\beta</math>/°</b>	110.063(10)	93.186(3)
<b><math>\gamma</math>/°</b>	74.017(10)	98.738(2)
<b>Volume/Å<sup>3</sup></b>	728.699	679.68(4)
<b>Z</b>	2	2
<b>Temperature/ K</b>	100	100

**Table 2** Unit cell parameters of form 1 and form 2

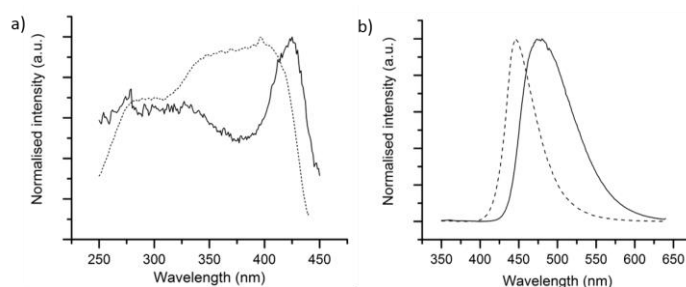


**Fig. 5** (a) Absorption and (b) emission spectra of Br-FN crystals of form 1 (dotted lines) and form 2 (solid lines).

Optical absorption measurements performed on crystals of form 1 and form 2 (Fig. 5) display peaks at 328 and 425 nm respectively. Form 1 has a fluorescence emission peak at 441 nm, and form 2 at 476 nm. The crossover point between the absorption and emission spectra, indicating the energy of the 0-0 transition, is at 430 nm for form 1 and 445 nm for form 2. Greater overlap between  $\pi$  bonds causes the formation of excimers, excitons delocalised over 2 molecules that shift emission to lower energies. Excimers also quench fluorescence, reducing emission efficiency<sup>19</sup>. This would explain why form 2 emits at lower energy and with less intensity compared to form 1. The differences in fluorescence intensity clearly illustrate the deleterious effect of  $\pi$ -stacking on the efficiency of fluorescence in organic crystals.

## Conclusions

Crystals of bis(4-bromophenyl)fumaronitrile have been grown via solution and physical vapour transport, with two distinct polymorphs being grown from the vapour phase, one of which was previously unknown. Lattice energy calculations suggest that this form has greater thermodynamic stability compared to the previously known form, with the previously known form crystallising at higher temperature within the PVT growth tube due to the release of binding energy of intermolecular interactions during the growth process. The new form was found to exhibit weaker red-shifted fluorescence emission to the conventional polymorph due to greater intermolecular  $\pi$ - $\pi$  overlap. These experiments demonstrate proof of the influence of  $\pi$ - $\pi$  interactions on the optical properties of organic crystals, and will help in elucidating the mechanisms of polymorphic control of crystals grown via physical vapour transport, showing that careful selection of growth conditions can be used to produce desired forms, potentially leading to the fabrication of crystals for high-efficiency optoelectronic devices.

## Acknowledgements

S.R.H., J.P. and T.T.J. acknowledge the Engineering and Physical Sciences Research Council UK (grants EP/G036780/1 and EP/L015544/1), and the Centre for Doctoral Training in Condensed Matter Physics and the Bristol Centre for Functional Nanomaterials for project funding. In addition, S.R.H. and L.T. would like to thank the support of the USAF European Office of Aerospace Research and Development (FA8655-12-1-2078). J.G.B. acknowledges support by the Alexander von Humboldt foundation within the Feodor-Lynen program and thanks Sally L. Price for helpful discussions. All authors thank Dr George Whittell of the University of Bristol for performing DSC, and Dr Hazel Sparkes for low temperature XRD data collection. T.T.J. would also like to thank Charlie Hall for insightful discussions and assistance with collecting experimental data, and Dr Hazel Sparkes and Dr Natalie Pridmore for assistance with SC-XRD data refinement.

## Conflicts of interest

There are no conflicts to declare.

## References

- Jiang H, Kloc C. Single-crystal growth of organic semiconductors. *MRS Bull.* 2013;38(1):28-33. doi:10.1557/mrs.2012.308.
- Reese C, Bao Z. Organic single-crystal field-effect transistors. *Mater Today.* 2007;10(3):20-27. doi:10.1016/S1369-7021(07)70016-0.
- Yeh HC, Wu WC, Wen YS, Dai DC, Wang JK, Chen CT. Derivative of  $\alpha,\beta$ -dicyanostilbene: Convenient precursor for the synthesis of diphenylmaleimide compounds, E-Z isomerization, crystal structure, and solid-state fluorescence. *J Org Chem.* 2004;69(19):6455-6462. doi:10.1021/jo049512c.
- Hong Y, Lam JWY, Tang BZ. Aggregation-induced emission. *Chem Soc Rev.* 2011;40(11):5361. doi:10.1039/c1cs15113d.
- Bruker, SAINT+ Integration Engine, Data Reduction Software, Bruker Analytical X-ray Instruments Inc., Madison, WI, USA, 2007.2007.
- Bruker, SADABS, Bruker AXS area detector scaling and absorption correction, Bruker Analytical X-ray Instruments Inc., Madison, Wisconsin, USA, 2001.
- Palatinus L, Chapuis G. SUPERFLIP - A computer program for the solution of crystal structures by charge flipping in arbitrary dimensions. *J Appl Crystallogr.* 2007;40(4):786-790. doi:10.1107/S0021889807029238.
- Palatinus L, Prathapa SJ, Van Smaalen S. EDMA: A computer program for topological analysis of discrete electron densities. *J Appl Crystallogr.* 2012;45(3):575-580. doi:10.1107/S0021889812016068.
- Sheldrick GM. A short history of SHELX. *Acta Crystallogr Sect A Found Crystallogr.* 2007;64(1):112-122. doi:10.1107/S0108767307043930.
- Dolomanov O V., Bourhis LJ, Gildea RJ, Howard JAK, Puschmann H. OLEX2: A complete structure solution, refinement and analysis program. *J Appl Crystallogr.* 2009;42(2):339-341. doi:10.1107/S0021889808042726.
- Dovesi R, Orlando R, Erba A, et al. CRYSTAL14 : A program for the ab initio investigation of crystalline solids. *Int J Quantum Chem.* 2014;114(19):1287-1317. doi:10.1002/qua.24658.
- Brandenburg JG, Caldeweyher E, Grimme S, et al. Screened exchange hybrid density functional for accurate and efficient structures and interaction energies. *Phys Chem Chem Phys.* 2016;18(23):15519-15523. doi:10.1039/C6CP01697A.
- Perdew JP, Burke K, Ernzerhof M. Generalized Gradient Approximation Made Simple. *Phys Rev Lett.* 1996;77(18):3865-3868. doi:10.1103/PhysRevLett.77.3865.
- Grimme S, Antony J, Ehrlich S, Krieg H. A consistent and accurate *ab initio* parametrization of density functional dispersion correction (DFT-D) for the 94 elements H-Pu. *J Chem Phys.* 2010;132(15):154104. doi:10.1063/1.3382344.
- Kresse G, Furthmüller J. Efficiency of ab-initio total energy calculations for metals and semiconductors using a plane-wave basis set. *Comput Mater Sci.* 1996;6(1):15-50. doi:10.1016/0927-0256(96)00008-0.

16. Stevens LA, Goetz KP, Fonari A, et al. Temperature-mediated polymorphism in molecular crystals: The impact on crystal packing and charge transport. *Chem Mater*. 2015;27(1):112-118. doi:10.1021/cm503439r.
17. Laudise R., Kloc C, Simpkins P., Siegrist T. Physical vapor growth of organic semiconductors. *J Cryst Growth*. 1998;187(3-4):449-454. doi:10.1016/S0022-0248(98)00034-7.
18. Wang H, Zhao Y, Xie Z, Wang H, Wang B, Ma Y. The thermodynamic characteristics of organic crystal growth by physical vapor transport: towards high-quality and color-tunable crystal preparation. *CrystEngComm*. 2014;16(21):4539-4545. doi:10.1039/C3CE42367K.
19. Ye K, Wang J, Sun H, et al. Supramolecular structures and assembly and luminescent properties of quinacridone derivatives. *J Phys Chem B*. 2005;109(16):8008-8016. doi:10.1021/jp0444767.